

30 **Abstract**

31 Osteoarthritis (OA) of the hip is a common and debilitating painful joint disease. A growing
32 body of evidence suggests that there may be an association between periarticular myotendinous
33 pathology and the development of hip OA. Thus, we hypothesized that a murine model of hip
34 OA could be achieved through selective injury of the abductor complex around the hip.
35 C57BL6/J mice were randomized to sham surgery or abductor injury, in which the myotendinous
36 insertion at the third trochanter and greater trochanter were surgically detached. Mice were
37 allowed free, active movement until sacrifice at either 3 weeks or 20 weeks post-injury.
38 Histologic analyses and immunohistochemical staining (IHC) of the femoral head articular
39 cartilage were performed, along with μ CT analysis to assess subchondral bone remodeling. We
40 observed that mice receiving abductor injury exhibited significant OA severity with loss of Type
41 II Collagen staining compared to sham control mice at 20 weeks post-surgery, comparable
42 MMP13 expression was observed between injury and sham groups. No significant differences
43 in subchondral bone were found on μ CT after 20 weeks following injury. Our study suggests a
44 link between abductor dysfunction and the development of hip OA, which are common
45 pathomorphologies encountered in routine orthopaedic clinical practice. Further, this novel
46 animal model may provide a valuable tool for future investigations into the pathogenesis and
47 treatment of hip OA.

48

49

50

51 **Introduction**

52 Osteoarthritis (OA) affects over 32.5 million people in the United States, and approximately 10%
53 of adults over the age of 45 will suffer from symptomatic hip OA at some point in their life¹. The
54 hip is the second most commonly affected large joint, after the knee². Hip OA is generally
55 divided into primary idiopathic causes, and secondary causes resulting from an identifiable
56 factor³. Secondary degeneration of the hip can result from a number of pathologies, including
57 inflammatory diseases such as rheumatoid arthritis, and has been linked to structural
58 pathomorphologies such as femoral acetabular impingement (FAI)⁴. Despite much study on the
59 causative factors related to the onset and progression of hip OA, the underlying etiology remains
60 to be elucidated.

61
62 The hip is a diarthrodial joint that allows for multidirectional range of motion. The periarticular
63 musculature of the hip, in particular the gluteus medius and minimus and their associated
64 tendons, contribute to dynamic stability of the joint. It is well-recognized that altered
65 arthrokinematics negatively influence articular cartilage loading and contributes to the
66 progression of OA. Multiple studies have observed an association between periarticular
67 tendinopathy and hip OA, without definitively establishing causality^{5,6}. In a clinical study, a
68 small series of patients with abductor tears were found to demonstrate a high rate of concomitant
69 intra-articular injury⁷. Therefore, these studies provided rationale for considering whether
70 musculotendinous dysfunction or injury surrounding the hip may lead to the development of OA.

71
72 Animal models of pathogenesis of hip joint and OA mostly utilize large animals including
73 canines⁸⁻¹⁰, sheep¹¹, and porcine¹² with the advantage of large animals having similar cartilage
74 morphology, thickness as well as the responses to injury to humans¹³⁻¹⁵. These large animal hip

75 OA models not only have already provided us invaluable insights into hip cartilage physiology
76 and pathophysiology but also serve as essential pre-clinical models for drug development.
77 Despite these benefits, large animals are not amenable to the power of genetic modification to
78 better define the cellular and molecular etiology of pathogenesis, as can be conducted in mice¹⁵.
79 Furthermore, there is a paucity of literature on murine hip injury models¹⁶. The purpose of the
80 present study, therefore, was to establish a novel murine model of hip OA induced by abductor
81 injury and determine whether an association exists between abductor insufficiency and hip OA
82 onset and progression. We hypothesize that abductor injury accelerates the development of hip
83 OA. OA severity, subchondral bone remodeling, as well as anabolic and catabolic biomarkers
84 were evaluated by histology, immunohistochemistry (IHC) and uCT analyses in the current
85 study.

86

87 **Materials and Methods**

88 *Animal Model of Abductor Instability*

89 All animal procedures were approved by the University Committee on Animal Research
90 (UCAR) at the University of Rochester. Female C57BL/6J mice (8-10 weeks-old; #00664,
91 Jackson Laboratories, Bar Harbor, ME) weighing on average between 20 and 25 g were
92 anesthetized by intraperitoneal injection of ketamine (60 mg/kg) and xylazine (4 mg/kg). The
93 hind region and right leg were shaved and prepared with alcohol and betadine (povidone-iodine).
94 The proximal femur was approached through a 1 cm lateral skin incision placed over the third
95 trochanter, followed by a direct incision through the fascial layer, exposing the underlying third
96 and greater trochanters.

97

98 Mice were randomly divided into two groups. One group received abductor injury, while the
99 other group received sham surgery. The effect of abductor injury on hip OA development was
100 investigated at two time points following surgery: 3 weeks and 20 weeks post-surgery. n = 4-5
101 mice per group (sham or surgery) per time point. The sham group underwent anesthesia along
102 with incisions of the skin and fascia. A Schematic diagram of the right proximal femur shows the
103 locations of the femoral head (FH), greater trochanter (GT), lesser trochanter (LT), third
104 trochanter (3T), and sciatic nerve (SN) (**Fig. 1A**). Coronal μ CT reconstruction of the right hip
105 demonstrates the anatomic positions of the FH and GT (**Fig. 1B**). The injury group had release
106 of the muscular attachments to the 3T (**Fig. 1C**) as well as detachment of the large abductor
107 complex (ABD) from the GT (**Fig. 1D**). During each surgery, careful attention was paid to avoid
108 injury to the SN running posterior to the proximal femur. For all mice, the fascial layer was
109 closed with a single 5-0 nylon suture (Ethicon, Inc.), and the skin was closed with either 7 mm
110 stainless steel wound clips (CellPoint Scientific Inc., Gaithersburg, MD) or a series of interrupted
111 5-0 nylon sutures. For analgesia, mice were given subcutaneous buprenorphine (0.05 mg/kg) at
112 the time of surgery and each subsequent day over the following 72 hours. Following surgery,
113 mice were returned to their cage and allowed free active motion and weight bearing. Animals
114 were monitored daily until sacrifice.

115

116 *Evaluation of bone tomography*

117 Mice were sacrificed at either 3-weeks or 20-weeks post-surgery (n = 4 -5 per group per time
118 point). Immediately after sacrifice, the hemi-pelvis and femur were prepared by removing the
119 skin and excess soft tissue, leaving the hip and the major muscular attachments around the pelvis
120 and femur. The samples were fixed for 72 hours in 10% neutral buffered formalin (NBF), then
121 washed, placed in 70% EtOH, and subjected to the μ CT scanning. Hips were scanned using the

122 VivaCT 40 system (Scanco Medical, Basserdorf, Switzerland) at highest resolution with a pixel
123 size of 10.5 μm to image bone. An integration time of 300 ms and an X-ray voltage of 55 kVP
124 was used. The hip was captured and segmented using a scanning threshold of 320 to identify
125 bone. The femoral head was analyzed for trabecular bone (excluding cortical) at a threshold of
126 310. Views of the femoral head and acetabulum were analyzed using a threshold of 320. The
127 Gaussian method was used for noise reduction (sigma 0.8 with support value of 1 pixel).

128

129 *Evaluation of OA severity*

130 Following 72 hours fixation and μCT scanning, samples were decalcified in 14% (pH 7.2)
131 EDTA at room temperature for 2 weeks. Samples were then dehydrated and embedded in
132 paraffin with the posterior surface of the hip facing down. Using the SN as a landmark, serial
133 sections (thickness = 5 μm) were taken through the preserved hip and surrounding soft tissue in a
134 coronal plane. Three different levels were cut through the joint, with five sections taken at each
135 level.

136

137 Safranin O / Fast Green staining was used to visualize changes in the hip articular structure and
138 proteoglycan content of the mice at 3 weeks and 20 weeks post-surgery. Slides were baked
139 overnight at 60°C, then deparaffinized and rehydrated through graded ethanol. After air drying,
140 slides were stained in Weigert's Hematoxylin for 7 minutes (Equal parts Solution A, CAS# 517-
141 23-2 and Solution B, CAS# 7705-08-0) then rinsed with running tap water. Slides were stained
142 with 0.02% Fast Green (CAS# 2353-45-9) for 3 minutes, rinsed in 1% acetic acid for 10 seconds,
143 then stained with 1% Safranin O (CAS# 477-23-6) for 5 minutes. After a quick rinse in 0.5%
144 acetic acid and rinses with double-distilled water, slides were then air dried and cover slipped.

145

146 OA severity was determined by modified Mankin scoring system as previously described¹⁷.
147 Three independent, blinded graders assessed sections for degenerative changes in the hip
148 articular cartilage. Scores including articular structure (0-11), tidemark (0-3), loss of
149 proteoglycan staining (0-8), and chondrocyte clones (0-2) were averaged among graders for the
150 hip femoral head, resulting in total scores between 0 and 24.

151

152 ***Immunohistochemistry***

153 Immunohistochemistry (IHC) was performed for Collagen Type II A1 (COL2A1) and Matrix
154 Metalloproteinase 13 (MMP13). For both protocols, slides were baked overnight at 60°C, then
155 deparaffinized and rehydrated through graded alcohols. IHC labeling for MMP13 (Thermo
156 Fischer Scientific, Waltham, MA. Catalog #MS-825P) began with enzymatic antigen retrieval
157 using hyaluronidase (Sigma-Aldrich, St. Louis, MO; H-3506) for 10 minutes in a 37°C water
158 bath. Endogenous peroxidase was then quenched for 30 minutes using endogenous blocking
159 reagent (Dako North America, Carpinteria, CA; S2003). After rinses with deionized water and
160 PBS-T, slides were blocked for 30 minutes with 5% Normal Horse Serum (NHS; Vectastain
161 Elite ABC Kit (Mouse IgG), Vector Laboratories, Burlingame, CA; PK-6102), then with the
162 Blocking Endogenous Antibody Technology (BEAT) kit (Invitrogen Corporation, Camarillo,
163 CA; 50-300). Overnight incubation with the primary antibody (Thermo Fischer Scientific,
164 Waltham, MA; MS-825P; 1:200) was done at 4°C, with control slides incubated with mouse IgG
165 at the same concentration (1µg/mL). On the second day, sections were incubated with the
166 secondary antibody (Vector PK-6102), then ABC reagent (Vector PK-6102). Color was detected
167 using Vector DAB ImmPACT kit (Vector SK-4105), then counterstained with hematoxylin.

168

169 IHC labeling for COL2A1 was performed as follows. Enzymatic antigen retrieval was performed
170 for 10 minutes in a 37°C water bath using pepsin (Sigma-Aldrich, P7000). After rinses, sections
171 were blocked with endogenous blocking reagent (Dako, S2003) for 30 minutes, then with 5%
172 NHS (Vector PK-6102) for 30 minutes. The primary antibody (Thermo Scientific, MS235-P;
173 1:100) was left to incubate at 4°C overnight, with control slides incubated with the same
174 concentration of mouse IgG (2ug/mL). On the second day, sections were incubated with the
175 secondary antibody (Vector PK-6102) and ABC reagent (Vector PK-6102), then color was
176 detected with the Vector DAB ImmPACT kit (Vector SK-4105) counterstained with
177 hematoxylin.

178

179 ***Statistics***

180 To determine how surgery, time (following surgery), and their interaction (surgery x time)
181 affected hip OA severity, as well as subchondral bone remodeling, data were analyzed by two-
182 way repeated measures ANOVA following by Sidak's multiple comparisons test ($\alpha = 0.05$) using
183 GraphPad Prism version 9. Values are expressed as mean \pm SD.

184

185 ***Source of Funding***

186 This study was supported by NIH AR075899 (CLW), OREF Etiology of Hip Osteoarthritis
187 Grant (CLW & BG) as well as Goldstein Award (BG) through the University of Rochester's
188 Department of Orthopaedics and Rehabilitation. MBG was supported by CTSA (TL1 TR000096)
189 from NIH/NCATS. CAO was supported by the University of Rochester Office for Medical
190 Education Year-Out Research Fellowship. The HBMI and BBMTI cores are supported by
191 NIH/NIAMS P30 AR069655.

192

193 **Results**

194 *Mice receiving abductor surgery demonstrated significantly increased OA severity compared*
195 *to sham group 20 weeks following injury.*

196 Safranin-O is a cationic dye that stains proteoglycans, and intensity of red Safranin-O staining is
197 a proxy for proteoglycan content. Loss of proteoglycan content is a clinical hallmark of OA¹⁸.
198 Hips from the sham and injured groups were stained at 3 weeks and 20 weeks post-injury with
199 Safranin-O/Fast Green to visualize proteoglycans. After 20 weeks, mice in the injured group
200 demonstrated loss of proteoglycan staining of the articular surface relative to sham, although
201 articular cartilage surface was comparable between two groups (**Fig. 2A-B**). No significant
202 differences in OA severity was observed between sham and injured groups at 3 weeks post-
203 injury. Furthermore, sham mice had similar OA severity at 3 weeks and 20 weeks post-surgery.

204

205 *Mice receiving abductor surgery exhibited decreased COL2A1 staining but comparable*
206 *MMP13 staining in the articular cartilage relative to sham mice at 20 weeks following*
207 *abductor injury*

208 IHC labeling for COL2A1 and MMP13 in articular cartilage of the femoral head was performed
209 at 20 weeks post-injury as this was the timepoint when OA was evident in the mice receiving
210 surgery. In the sham group, a superficial layer of unmineralized cartilage is characterized by
211 pericellular staining of COL2A1 (**Fig. 3A-B**). In the deeper layers, staining intensity is increased
212 and more evenly distributed throughout the extracellular matrix. Hips from the injury group
213 show a notable decrease in staining intensity in the uncalcified articular cartilage, relative to
214 sham mice.

215 MMP13 has been shown to play a catabolic role in OA¹⁹, and increased staining of MMP13 has
216 been observed in animal models of arthritis^{20,21}. IHC staining for MMP13 was performed to

217 visualize changes in femoral head articular cartilage after sham surgery and abductor injury.
218 There was no appreciable staining for MMP13 in the articular cartilage at 20 weeks post-injury
219 in the both sham and surgery groups (**Fig. 3**).

220

221 ***μCT reveals no significant change in subchondral bone parameters 20 weeks post-injury***

222 To evaluate potential structural changes in subchondral bone, hips from the sham group and the
223 injury group were analyzed by μCT to compare subchondral microtrabecular volumetric
224 parameters 3- and 20-weeks following injury (**Fig. 4**). No changes in cancellous bone fraction
225 (bone volume/total volume, BV/TV, excluding the cortex) were detected in the injured group
226 relative to sham at 20 weeks (Sham: 0.51 ± 0.1 ; Injury: 0.51 ± 0.1) (**Fig. 4A**). In addition, there
227 were no significant differences in trabecular bone characteristics between two groups. This
228 includes trabecular number (Sham: $6.3/\text{mm} \pm 0.8$; Injury: $6.3/\text{mm} \pm 0.4$) (**Fig. 4B**), trabecular
229 thickness (Sham: $79.2 \mu\text{m} \pm 8.1$; Injury: $81.8 \mu\text{m} \pm 7.3$) (**Fig. 4C**), and trabecular spacing (Sham:
230 $151.8 \mu\text{m} \pm 23.5$; Injury: $147.5 \mu\text{m} \pm 10.8$) (**Fig. 4D**).

231

232 **Discussion**

233 With the growth in clinical evidence indicating an association between abductor insufficiency
234 and the development of hip OA, it is essential to develop a reproducible small animal model that
235 allows scientists to study the pathogenesis of this linked disease process^{5,6}. To date, however,
236 only a few rodent hip OA models have been established and can be generally categorized into
237 either chemically-induced or surgically-induced OA^{16,22}. Intra-articular injection of monosodium
238 Iodoacetate (a chondrocyte glycolytic inhibitor) exhibited rapid hip OA development compared
239 to controls within 14 days in a rat model. However, it is not clear whether such a progressive and
240 destructive OA phenotype is representative of chronic hip OA in humans²². In another study,

241 various degrees of hip instability ranging from mild, moderate, severe to femoral head resection
242 were surgically induced in mice at weaning (3-week-old neonatal pups)¹⁶. Their data suggest that
243 hip instability induced by loss-of-function of soft connective tissue led to morphometric changes
244 in the growing mouse hip. However, understanding how abductor injury may induce OA in the
245 context of a skeletally mature hip (as indicated fusion of triradiate cartilage of the pelvis)²³, has
246 remained a key knowledge gap to this point. Furthermore, our small animal hip OA model may
247 be used to explore the sequence of pathoanatomical and anabolic/catabolic effects on OA onset
248 and progression.

249
250 Animal models of surgical OA require well-established techniques that can be easily
251 reproduced¹³. In this model the third trochanter (3T) serves as a surgical landmark, which can be
252 palpated before making the skin incision. Once the muscular attachments to the 3T have been
253 cut, the femur is followed proximally to the large abductor complex on the greater trochanter
254 (GT). These muscles are easily visualized, and can be cleanly cut without injuring surrounding
255 structures. The surgery avoids dissecting around deep structures; the major potential injury is to
256 the sciatic nerve (SN) running posterior to the proximal femur. In preliminary work, we
257 experimented with performing a capsulotomy to induce an even greater severity of injury.
258 Through multiple surgeries, we found that the capsule in the mouse may be too small to reliably
259 incise without risking damage to the sciatic nerve running in close approximation to the joint. As
260 such, this group has been excluded from the presented results.

261
262 The primary findings in this study were the loss of proteoglycan and COL2A1 staining in
263 uncalcified articular cartilage 20 weeks after injury. Loss of proteoglycan and type II collagen

264 contents are both histologic hallmarks of OA, and the observations made in the injured group
265 after 20 weeks suggest that OA progression is accelerated after abductor injury. Additionally,
266 sham mice had similar OA severity at 3 weeks and 20 weeks post-surgery, suggesting that both
267 sham surgery and aging (i.e. ~ 6 months of age) were not sufficient to induce hip OA onset.
268 Interestingly, no changes in MMP13 IHC staining were observed between the sham and injured
269 groups, suggesting that either MMP13 may not be the main catabolic mediator in our mouse hip
270 OA model or other timepoints may need to be investigated in order to establish temporal
271 expression pattern of MMP13. Indeed, our results are also consistent with the findings from the
272 study of Killian *et al.* where the authors indicated low MMP13 staining in articular cartilage in
273 their titrated model of hip dysplasia. Future studies investigating other cartilage degradation
274 enzymes, such as ADAMTS4, MMP3, MMP9, etc., as well as additional timepoints post-surgery
275 are warranted. Radiographic analysis of subchondral bone remodeling did not reveal significant
276 differences between sham and injured groups at any time point investigated in this study.
277 Nevertheless, long-term study may be required to observe subchondral bone remodeling in our
278 mouse model.

279
280 The gluteus medius and minimus, in conjunction with the tensor fascia lata and gluteus maximus,
281 represent the main components of the hip abductor complex. This complex contributes to the
282 “contractile layer” of the hip, and is thought to exert considerable influence on the intraarticular
283 joint space and its associated layers²⁴. In a clinical outcome study that evaluated the results of
284 arthroscopic gluteus medius/minimus repairs, a high incidence of concomitant intraarticular hip
285 pathology was noted⁷. Abductor tendon pathology leads to considerable pain and functional
286 impairment. Both open and arthroscopic repair techniques have been proposed and excellent

287 clinical results have been reported for both repair types^{7,25,26}. The causal relationship between
288 periarticular myotendinous pathology and the onset and progression of OA is intriguing but
289 remains understudied. Emerging clinical data for the hip joint support the association between
290 pathology of the extra-articular soft tissue envelope and intra-articular joint disease. Therefore,
291 reestablishment of an effective abductor force coupling mechanism may help to optimize and re-
292 balance loading characteristics and potentially influence the progression of intraarticular
293 degenerative changes that may ultimately result in the need for joint arthroplasty.

294
295 The true incidence of abductor tears and/or tendinosis in the general and athletic population
296 remains unknown. In addition, the natural history of untreated tears is unclear. Some studies
297 have observed an association between hip abductor disease and OA^{5,27}. A recent histologic study
298 evaluated the ultrastructure of the abductor tendon complex in 10 patients treated for displaced
299 femoral neck fractures and 10 patients undergoing total hip arthroplasty for OA. All of the
300 patients treated for OA were found to have coexisting tendinosis, with prominent scarring and
301 overall greater degenerative changes than the group treated for traumatic fractures of the femoral
302 neck⁶. While not clearly establishing that tendon pathology contributes to OA, these observations
303 raise important questions regarding the relationship between these two pathologies. It is likely
304 that abductor compromise, through an analogous pathomechanical process, may contribute to the
305 onset and progression of hip OA.

306
307 While our present study establishes a reproducible injured-induced mouse hip OA model and
308 offers an important step forward in investigating the role of abductor insufficiency in the
309 development of hip OA, there are limitations that must be considered. First, the mechanisms
310 underlying myotendinous pathology and abductor insufficiency leading to mouse hip OA

311 development remain to be determined. Particularly, to what extent the biomechanical loading on
312 the hip cartilage and mouse behaviors such as gaits and weight bearing are altered following
313 abductor surgery need to be quantified in the future. An additional limitation that must be
314 considered is the clinical relevance of a quadruped model for hip OA, as weight bearing is
315 distributed across four limbs in mice, and thus, gait and biomechanics differ from humans.
316 Despite this limitation, mice and humans share similar joint congruence at the hip.

317

318 In conclusion, we have established a novel murine model of surgically-induced hip OA through
319 an injury to the abductor complex around the hip. Furthermore, this model may be utilized as a
320 valuable tool to examine potential biomarkers associated with hip OA progression²⁸. We believe
321 that for the broader orthopaedic community of clinicians and researchers, our findings will
322 increase understanding the role of abductors in hip stability and the development of joint
323 pathology.

324

325 **Acknowledgements**

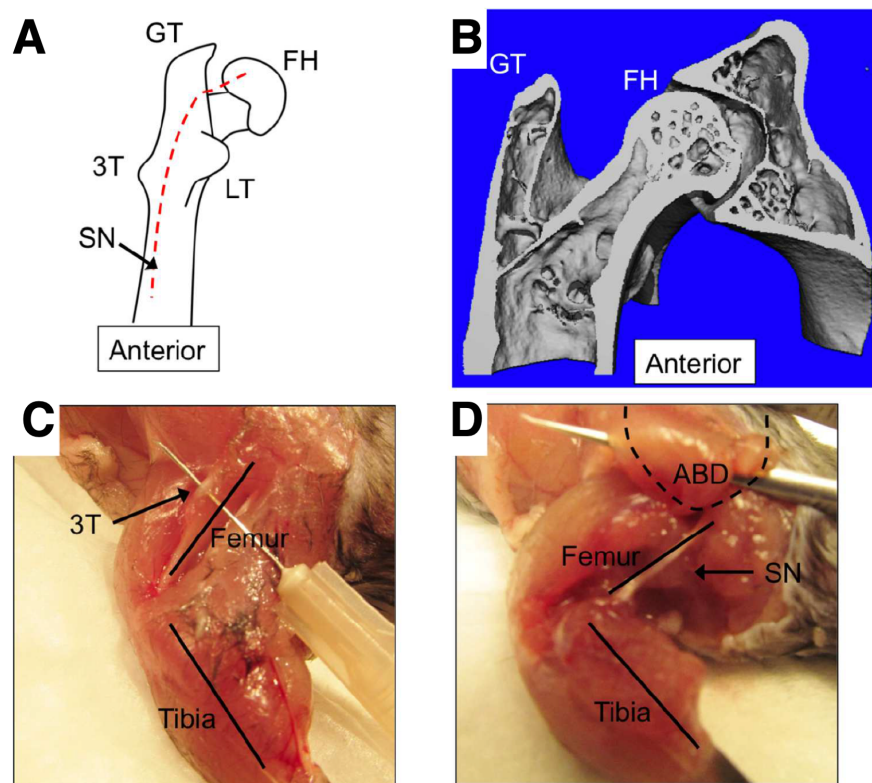
326 We would like to thank the Histology, Biochemistry and Molecular Imaging (HBMI) and
327 Biomechanics, Biomechanics and Multimodal Tissue Imaging (BBMTI) cores in the Center for
328 Musculoskeletal Research (CMSR) for technical assistance. We appreciate the gracious
329 generosity of the Goldstein Family, who supported the Goldstein Award which provided funding
330 for this work. We also thank Dr. Victoria Hansen and Gulzada Kulzhanova's assistance on
331 performing modified Mainkin score grading for hip joint OA severity for the current project.

332

333 **Author contributions**

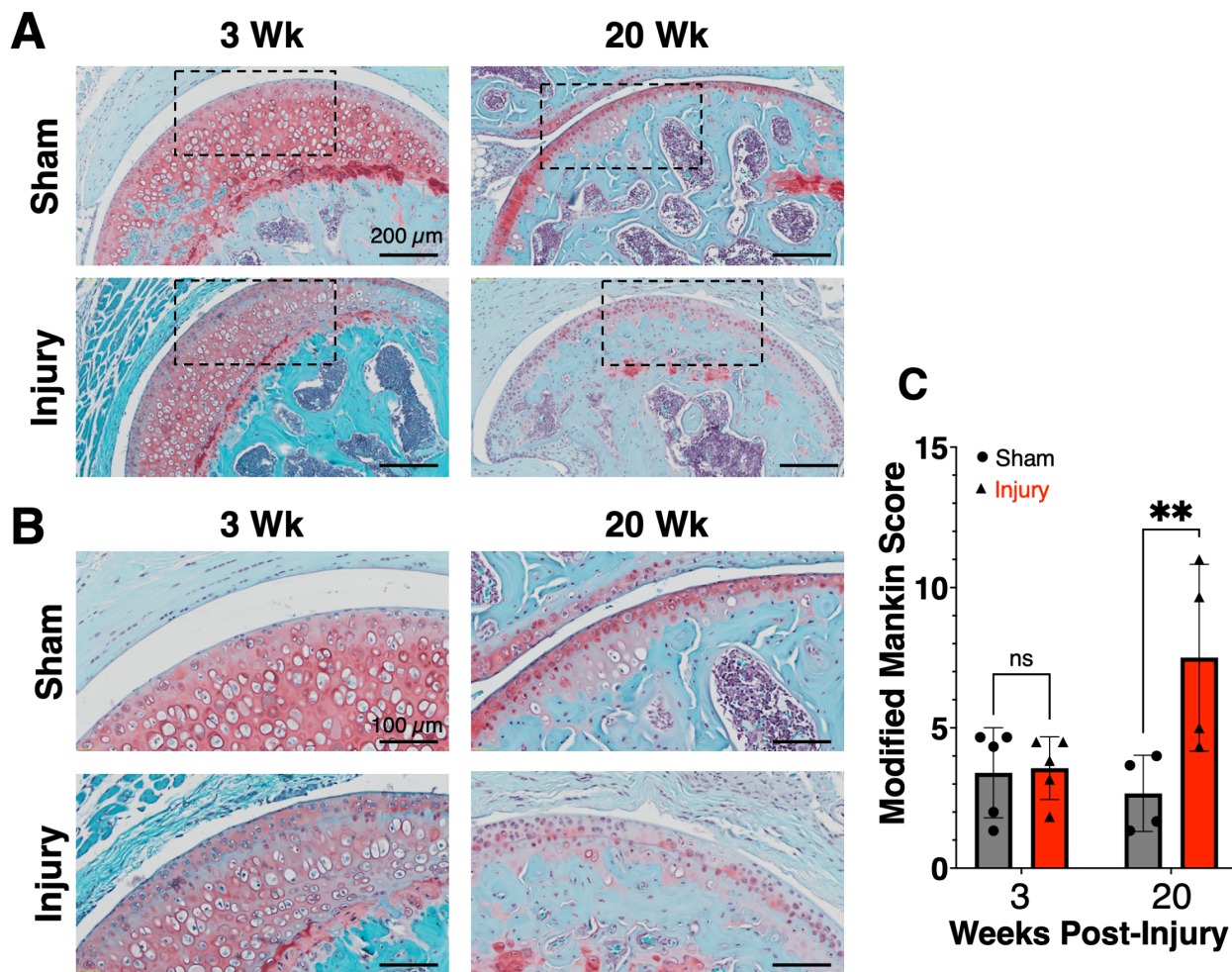
334 AL, CLW, and BG conceptualized the study. MBG and CAO performed mouse surgeries and
335 μ CT measurements. HS, CLW, and members in CLW's lab performed modified Mainkin score
336 grading for hip joint OA severity. HS performed IHC staining and imaging. All authors wrote,
337 reviewed, and edited the manuscript.

338 **Figure and Figure Legends**



339

340 **Figure 1. Surgical model of abductor complex injury.** (A) Schematic of the right proximal
341 femur showing the locations of the femoral head (FH), greater trochanter (GT), lesser trochanter
342 (LT), and third trochanter (3T), as well as the path of the sciatic nerve (SN) running posterior to
343 the femur. (B) Coronal reconstruction of the right hip showing the anatomic positions of the
344 femoral head (FH) and greater trochanter (GT). (C) Photograph of the left hind limb with skin
345 removed. The femur and tibia are labeled for orientation. The third trochanter (3T) is visible
346 superficially, with a needle placed into the muscular attachments. Attachments running proximal
347 from the third trochanter were removed in this injury model. (D) Photograph of the left hind limb
348 highlighting the abductor attachments (ABD) to the greater trochanter (dashed outline). The
349 entire abductor complex was detached in the injury group. The femur, tibia, and sciatic nerve
350 (SN) are labeled for orientation.



351

352 **Figure 2. Abductor injury results in loss of proteoglycan staining 20 weeks post-surgery.**

353 Coronal sections through the hip were stained with Safranin O/Fast Green, in which

354 proteoglycan stains red. (A) Sections are shown for sham and injured groups at 3 and 20 weeks

355 after surgery. Loss of proteoglycan staining is evident in the injured group after 20 weeks

356 relative to sham group. (B) Increased magnification of the areas indicated by dashed rectangles

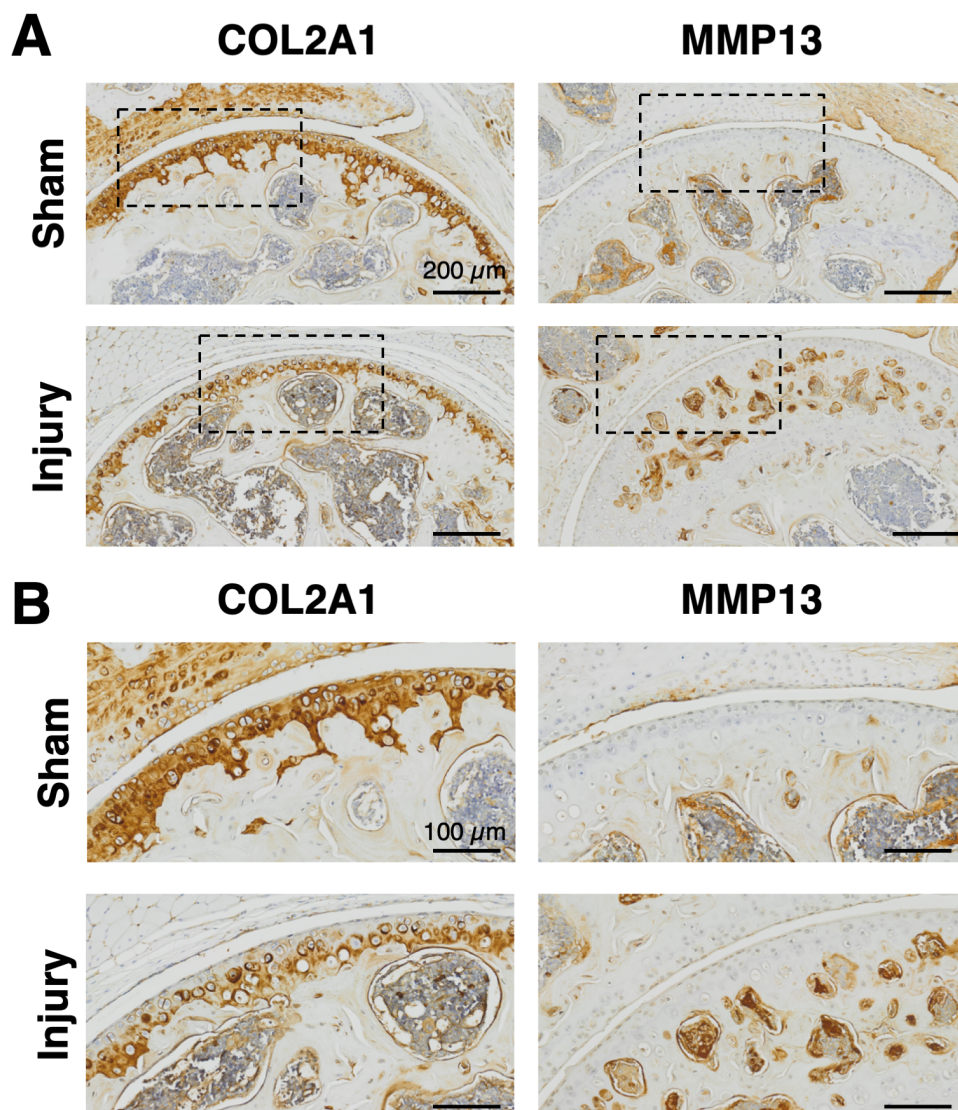
357 in (A). (C) Modified Mankin scores shows increased OA severity of the mice receiving surgery

358 20 weeks post-injury as compared to corresponding sham group. Two-way repeated measured

359 ANOVA following by Sidak's multiple comparisons test. Mean ± SD. ns: No statistically

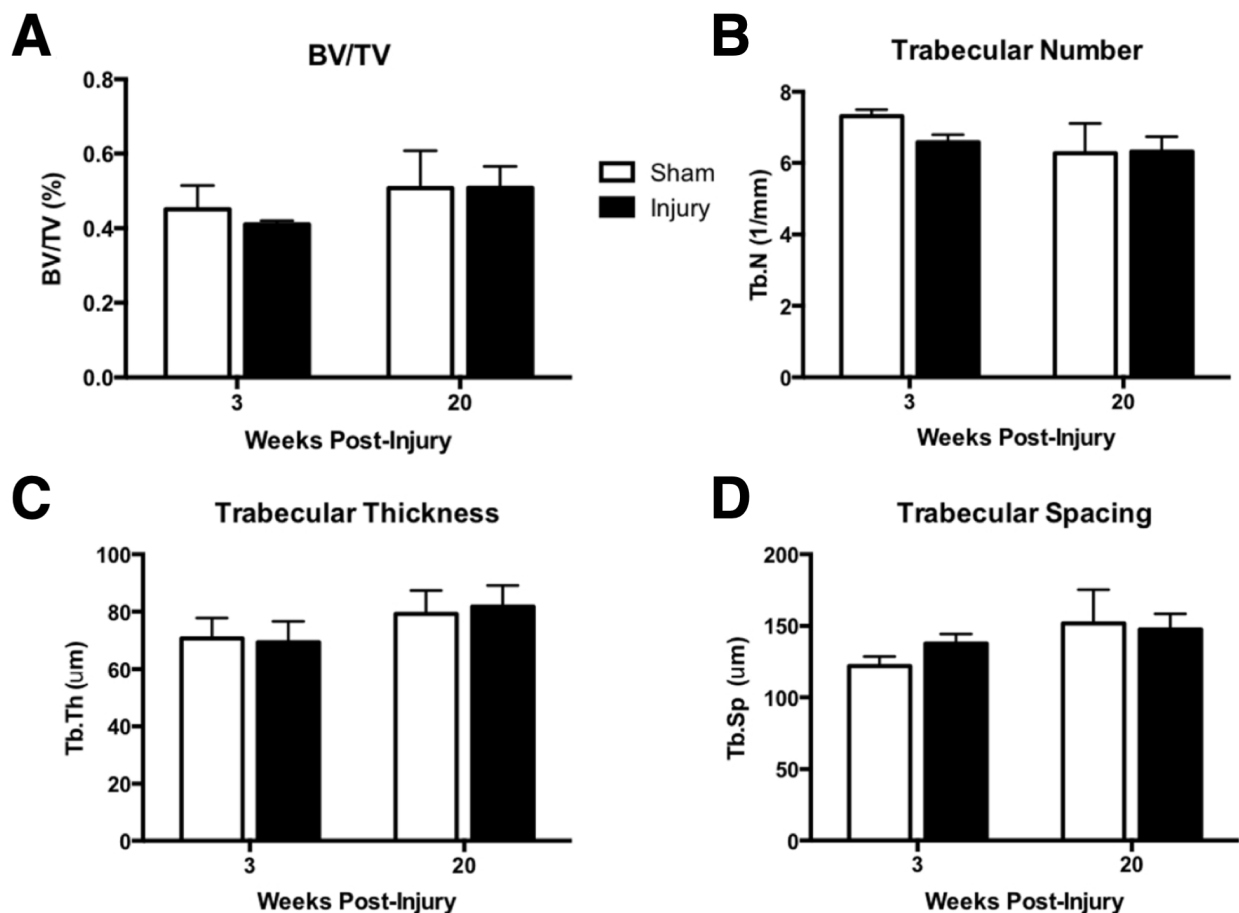
360 significant was detected.

361



362

363 **Figure 3. COL2A1 and MMP13 staining reveal loss of type II collagen content in the**
364 **unmineralized hip cartilage of the mice 20 weeks post-surgery. (A)** Coronal sections through
365 the hip are shown following IHC for COL2A1 and MMP13 staining. Dark red/brown color
366 indicates positive staining. A substantially decreased COL2A1 staining in the unmineralized hip
367 cartilage of the mice receiving surgery; however, no apparent staining for MMP13 was detected
368 for both sham and surgery groups. **(B)** Increased magnification of the areas indicated by dashed
369 rectangles in **(A)**.



370

371 **Figure 4. μCT analysis indicates no significant changes in subchondral bone parameters**

372 **following abductor injury.** μCT was used to assess the subchondral bone of the femoral head.

373 (A) The ratio of bone volume to total volume (BV/TV), (B) Trabecular number, (C) trabecular

374 thickness, and (D) trabecular spacing were measured at 3- and 20-weeks post-surgery for bot

375 sham and surgery groups. There are no significant differences in subchondral bone parameters

376 between the two groups in any time point investigated. Two-way repeated measured ANOVA

377 following by Sidak's multiple comparisons test. Mean ± SD.

378

379 **Reference**

- 380 1 Lawrence, R. C. *et al.* Estimates of the prevalence of arthritis and other rheumatic
381 conditions in the United States: Part II. *Arthritis & Rheumatism* **58**, 26-35 (2008).
- 382 2 Zhang, W. *et al.* OARSI recommendations for the management of hip and knee
383 osteoarthritis, part I: critical appraisal of existing treatment guidelines and systematic
384 review of current research evidence. *Osteoarthritis and cartilage* **15**, 981-1000 (2007).
- 385 3 Hoaglund, F. T. & Steinbach, L. S. Primary osteoarthritis of the hip: etiology and
386 epidemiology. *JAAOS-Journal of the American Academy of Orthopaedic Surgeons* **9**,
387 320-327 (2001).
- 388 4 Elias-Jones, C. J. *et al.* Inflammation and neovascularization in hip impingement: not just
389 wear and tear. *The American journal of sports medicine* **43**, 1875-1881 (2015).
- 390 5 Howell, G., Biggs, R. & Bourne, R. Prevalence of abductor mechanism tears of the hips
391 in patients with osteoarthritis. *The Journal of arthroplasty* **16**, 121-123 (2001).
- 392 6 Meknas, K. *et al.* Could tendinosis be involved in osteoarthritis? *Scandinavian journal of*
393 *medicine & science in sports* **22**, 627-634 (2012).
- 394 7 Domb, B. G., Botser, I. & Giordano, B. D. Outcomes of endoscopic gluteus medius
395 repair with minimum 2-year follow-up. *The American journal of sports medicine* **41**, 988-
396 997 (2013).
- 397 8 Pascual - Garrido, C. *et al.* Canine hip dysplasia: a natural animal model for human
398 developmental dysplasia of the hip. *Journal of Orthopaedic Research®* **36**, 1807-1817
399 (2018).
- 400 9 Little, D. *et al.* Functional outcome measures in a surgical model of hip osteoarthritis in
401 dogs. *Journal of experimental orthopaedics* **3**, 1-16 (2016).

- 402 10 Jónasson, P. S. *et al.* Strength of the porcine proximal femoral epiphyseal plate: the effect
403 of different loading directions and the role of the perichondrial fibrocartilaginous
404 complex and epiphyseal tubercle—an experimental biomechanical study. *Journal of*
405 *experimental orthopaedics* **1**, 1-9 (2014).
- 406 11 Siebenrock, K. A., Fiechter, R., Tannast, M., Mamisch, T. C. & von Rechenberg, B.
407 Experimentally induced cam impingement in the sheep hip. *Journal of orthopaedic*
408 *research* **31**, 580-587 (2013).
- 409 12 Pawaskar, S. S., Grosland, N. M., Ingham, E., Fisher, J. & Jin, Z. Hemiarthroplasty of hip
410 joint: An experimental validation using porcine acetabulum. *Journal of biomechanics* **44**,
411 1536-1542 (2011).
- 412 13 Teeple, E., Jay, G. D., Elsaid, K. A. & Fleming, B. C. Animal models of osteoarthritis:
413 challenges of model selection and analysis. *The AAPS journal* **15**, 438-446 (2013).
- 414 14 Gregory, M. H. *et al.* A review of translational animal models for knee osteoarthritis.
415 *Arthritis* **2012** (2012).
- 416 15 Oláh, T., Michaelis, J. C., Cai, X., Cucchiarini, M. & Madry, H. Comparative anatomy
417 and morphology of the knee in translational models for articular cartilage disorders. Part
418 II: Small animals. *Annals of Anatomy-Anatomischer Anzeiger* **234**, 151630 (2021).
- 419 16 Killian, M. L. *et al.* Novel model for the induction of postnatal murine hip deformity.
420 *Journal of Orthopaedic Research®* **37**, 151-160 (2019).
- 421 17 Wu, C.-L. *et al.* Dietary fatty acid content regulates wound repair and the pathogenesis of
422 osteoarthritis following joint injury. *Annals of the rheumatic diseases* **74**, 2076-2083
423 (2015).

- 424 18 Schmitz, N., Laverty, S., Kraus, V. & Aigner, T. Basic methods in histopathology of joint
425 tissues. *Osteoarthritis and cartilage* **18**, S113-S116 (2010).
- 426 19 Wang, M. *et al.* MMP13 is a critical target gene during the progression of osteoarthritis.
427 *Arthritis research & therapy* **15**, 1-11 (2013).
- 428 20 Shen, J. *et al.* Deletion of the transforming growth factor β receptor type II gene in
429 articular chondrocytes leads to a progressive osteoarthritis - like phenotype in mice.
430 *Arthritis & Rheumatism* **65**, 3107-3119 (2013).
- 431 21 Roach, H. I. *et al.* Association between the abnormal expression of matrix - degrading
432 enzymes by human osteoarthritic chondrocytes and demethylation of specific CpG sites
433 in the promoter regions. *Arthritis & Rheumatism: Official Journal of the American*
434 *College of Rheumatology* **52**, 3110-3124 (2005).
- 435 22 Kawarai, Y. *et al.* Changes in proinflammatory cytokines, neuropeptides, and microglia
436 in an animal model of monosodium iodoacetate - induced hip osteoarthritis. *Journal of*
437 *Orthopaedic Research*[®] **36**, 2978-2986 (2018).
- 438 23 Ford, C. A., Nowlan, N. C., Thomopoulos, S. & Killian, M. L. Effects of imbalanced
439 muscle loading on hip joint development and maturation. *Journal of Orthopaedic*
440 *Research* **35**, 1128-1136 (2017).
- 441 24 Draovitch, P., Edelstein, J. & Kelly, B. T. The layer concept: utilization in determining
442 the pain generators, pathology and how structure determines treatment. *Current reviews*
443 *in musculoskeletal medicine* **5**, 1-8 (2012).
- 444 25 Bunker, T., Esler, C. & Leach, W. Rotator-cuff tear of the hip. *The Journal of Bone and*
445 *Joint Surgery. British volume* **79**, 618-620 (1997).

- 446 26 Kagan 2nd, A. Rotator cuff tears of the hip. *Clinical orthopaedics and related research*,
447 135-140 (1999).
- 448 27 Kingzett-Taylor, A. *et al.* Tendinosis and tears of gluteus medius and minimus muscles as
449 a cause of hip pain: MR imaging findings. *AJR. American journal of roentgenology* **173**,
450 1123-1126 (1999).
- 451 28 Nepple, J. J., Thomason, K. M., An, T. W., Harris-Hayes, M. & Clohisy, J. C. What is the
452 utility of biomarkers for assessing the pathophysiology of hip osteoarthritis? A systematic
453 review. *Clinical Orthopaedics and Related Research*® **473**, 1683-1701 (2015).
454